Journal of Photochemistry and Photobiology A: Chemistry 215 (2010) 31–37

Contents lists available at ScienceDirect

Journal of Photochemistry and Photobiology A: Chemistry

journal homepage: www.elsevier.com/locate/jphotochem

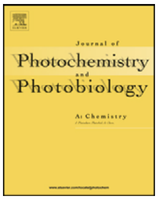

Solvent effect on photophysical properties and Mg^{2+} binding of 1,3-diphenyl-propane-1,3-dione

Tandrima Chaudhuri[a], Prashant Shukla[b], Sandip K. Nayak[b], Subrata Chattopadhyay[b], Manas Banerjee[c,*]

[a] Department of Chemistry, Dr. Bhupendra Nath Dutta Smriti Mahavidyalaya, Hatgobindapur, Burdwan 713407, India
[b] Bio-Organic Division, Bhabha Atomic Research Centre, Mumbai 400085, India
[c] Department of Chemistry, University of Burdwan, Burdwan 713104, India

ARTICLE INFO

Article history:
Received 27 January 2010
Received in revised form 19 June 2010
Accepted 20 July 2010
Available online 10 August 2010

Keywords:
β-Diketone
Solvatochromism
Mg^{2+} binding
H-bonded excited state

ABSTRACT

The absorption and emission spectroscopic investigations of a β-diketone, 1,3-diphenyl-propane-1,3-dione (**1k**) in various polar, non-polar as well as protic and aprotic solvents are reported. The solvatochromic shifts of the spectral bands were studied in a multitude of solvents followed by multilinear regression in which several solvent parameters were simultaneously analysed. This π-conjugated β-diketone exhibits solvatochromism. Variation in the electronic absorption and emission spectral characteristics of **1k** were studied in solution in presence of magnesium perchlorate. Absorption spectral studies indicate complex formation between magnesium ion and **1k** in the ground state. The values of equilibrium constant, enthalpy and entropy of complex formation together with the molar absorbance of the absorbing species have been determined for the diketone–cation 1:1 interaction. Fluorescence spectral changes with the addition of $Mg(ClO_4)_2$ revealed the existence of hydrogen bonded excited state of **1k**. The values of equilibrium constant for **1k**/Mg^{2+} interaction have been measured in acetone and methanol media.

1. Introduction

Modification of spectral behaviour of a dipolar solute on interacting with electrolytes has long been studied [1]. For the solute possesses charge separation either in the ground or in the excited state the effect is particularly more pronounced. Thus, the charge transfer (CT) bands of UV–vis probes are expected to exhibit electrolyte induced spectral changes. By observing the influence of solvent polarity on charge transfer (CT) transitions [2,3], the polarity parameters involving the maximum energy of absorption have been proposed for electrolyte solutions [3–5]. Attempts have been made to explain the spectral changes in terms of the electric field effect of the ion [6], but in many instances it has been found that the observed spectral changes are due to a change in speciation, rather than the non-specific electric field effect [7]. Emission studies, indicating the excited state properties, however, have been only little explored [8,9]. β-Diketones constitute a class of compounds which are characterized by solvent-dependent absorption and fluorescence properties [10]. β-Diketonate acceptors, for example, are classic ligands for the main group, transition metal and lanthanide series of elements [11]. Their complexes display a vast array of chemical and physical functions ranging from light emission [12] to molecular recognition [13] and catalysis [14]. Other reports have focused on diketone binding with Group II metals due to their importance in biology [15,16]. For example, diketo acid derivatives serve as antiviral Mg^{2+} chelate drug leads, given that Mg^{2+} is believed to be essential for the function of HIV integrase and hepatitis C polymerase in viral replication [17,18]. Although many optical detection methods for Mg^{2+} and Ca^{2+} have been developed [19,20], only few involve diketone for their binding.

Here, we have reported the solvatochromic properties of 1,3-Diphenyl-propane-1,3-dione (**1k** in Fig. 1). Interestingly, **1k** has highly π-conjugated rigid planar *cis*-enol emitting tautomer that contains bulky phenyl rings with both the keto groups. The objective of the present work is to investigate the effect of solvent environment on spectral properties of **1k** as well as of the complexed diketone (**1k**/Mg^{2+}). Here it has been observed that Mg^{2+} ion brings about a significant change in spectral properties of the **1k** in both protic and aprotic solvents. Further, a complex is formed between the cation and the diketone molecule in the ground (S_0). Solvents used were protic methanol (MeOH) and aprotic acetone (AC) for this interaction study. The modulation of emission of **1k** by solvent polarity and metal binding were explored.

---

* Corresponding author. Tel.: +91 3422656700; fax: +91 3422530452.
E-mail address: manasban@rediffmail.com (M. Banerjee).

1010-6030/$ – see front matter © 2010 Elsevier B.V. All rights reserved.
doi:10.1016/j.jphotochem.2010.07.017

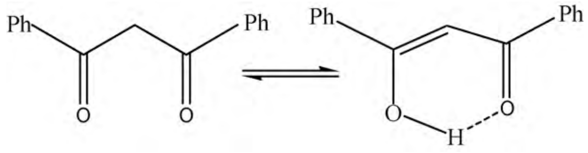

Fig. 1. Structure of the diketone (**1k**).

2. Experimental

2.1. Materials

The β-diketone, 1,3-diphenyl-propane-1,3-dione was prepared according to the reported method [21]. Purity of the prepared compound was checked by IR, absorption and fluorescence spectral measurements and also by thin layer chromatography. All the solvents (HPLC grade, Merck) were used without further purification. Magnesium perchlorate [Aldrich] was dried in oven before use. Samples were preserved in a dry box so as to avoid contamination from moisture.

2.2. Steady state spectral measurements

Absorption (UV–vis) spectral measurements were performed on a SHIMADZU UV 1601 PC spectrophotometer fitted with an electronic temperature controller unit (TCC–240 A). The steady state fluorescence emission and excitation spectra were recorded on a Hitachi F-4500 spectrofluorimeter equipped with a temperature controlled cell holder.

2.3. Time resolved fluorescence measurement

Fluorescence decay was studied by time correlated single photon counting (TCSPC) using the FLUOROCUBE lifetime system (IBH, s/n 04412). The detailed experimental set up were as follows: A nanoLED of 336 nm (IBH, UK, NanoLED-16, s/n 04937) was used as excitation source with FWHM of the order of 1.1 ns and the pulse was passed through 5000 M emission monochromator. The fluorescence signal was detected in magic angle polarization using cooled red-sensitive photocathode (TBX-04-A) detector with a response time of 180 ps. The decays were analysed using IBH DAS-6 decay analysis software. Intensity decay curves were then fitted with four-exponential decay expression. In the present work, the fluorescence intensity for the dye in pure solvents as a function of time t, $F(t)$ could be fitted with a four-exponential expression given by Eq. (1):

$$F(t) = \sum_{i=1}^{4} a_i \quad \exp\left(\frac{-t}{\tau_i}\right) \tag{1}$$

where a_i and τ_i are the amplitude and time constant, respectively, for the ith decay component.

3. Result and discussion

3.1. Photophysical study

The photophysical parameters [electronic absorption maxima (λ_{abs}), emission maxima (λ_{em}), fluorescence quantum yield (Φ_{fl}) and lifetime (τ_0)] of **1k** were determined in a few polar, non-polar and protic, aprotic solvents. The energy of maximum absorption $E(A)$, fluorescence $E(F)$ and Stoke's shift $E(\text{St})$ were reported through the relation:

$$E \quad (\text{kcal mol}^{-1}) = \frac{28590}{\lambda \quad (\text{nm})}$$

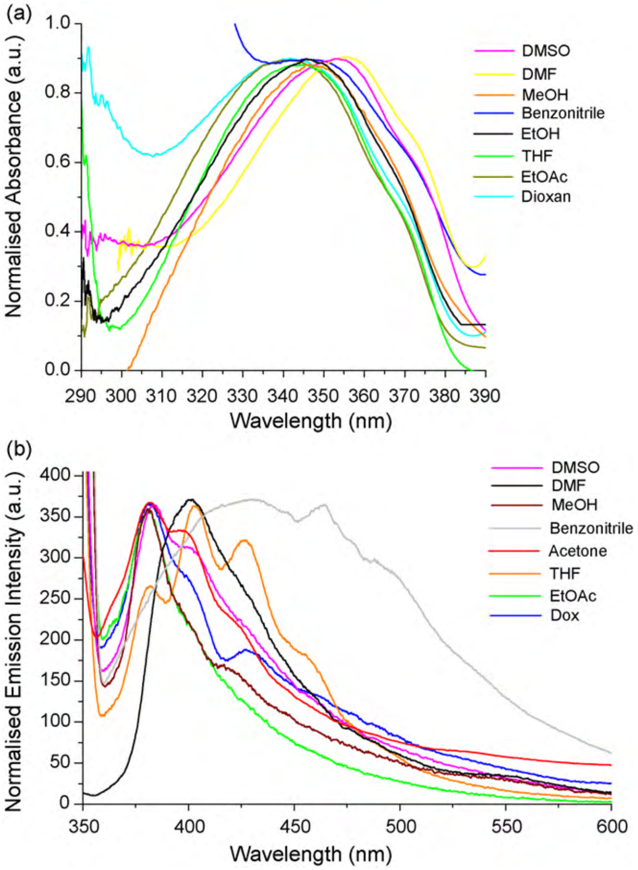

Fig. 2. (a) Absorption spectra of **1k** in different indicated solvents. (b) Fluorescence spectra of **1k** in different indicated solvents.

The measured $E(A)$ and $E(F)$ values for the diketone **1k** were given in Table 1. The diketone shows intense $S_0 \rightarrow S_1$ absorption at 353.40 nm, i.e. 80.90 kcal mol^{-1} in dimethyl sulphoxide (DMSO), and the absorption maxima were seen to be hypsochromically shifted by 1–16 kcal mol^{-1} in other solvents. For the steady state fluorescence, solvent-dependent shifts of the fluorescence maxima were correspondingly smaller in the respective solvents. In aprotic solvents the fluorescence band shows almost similar structure which looses their prominence as the polarity of the solvent is increased. The possible origin of structure of the band is presumably the carbonyl vibrations. The representative absorption and fluorescence spectra of the diketone in different solvents were shown in Fig. 2a and b respectively. In benzonitrile, **1k** showed an exceptional spectral behaviour in that the most intense absorption peak appeared at 306.20 nm, i.e. 93.37 kcal mol^{-1} together with that of 345.0 nm, i.e. 82.87 kcal mol^{-1} peak. Emission study showed a very broad bathochromically shifted peak maximum at 431.02 nm, i.e. 66.33 kcal mol^{-1} having the Stoke's shift of ~17 kcal mol^{-1}, i.e. 86.03 nm.

The maximum absorption energies $E(A)$ of **1k** expressed in kcal mol^{-1} for aprotic and protic solvents, show a linear correlation with the Reichardt parameter $E_T(30)$ [3], as was shown in Fig. 3a. A linear correlation with the $E_T(30)$ scale of solvent polarity is indicative of intramolecular charge transfer (ICT) accompanying the $S_0 \rightarrow S_1$ transition. The negative slope of $E(A)$ vs $E_T(30)$ plot in Fig. 3a indicated that the transition is accompanied by an increase in the dipole moment for the diketone **1k**, while the reverse is true for the indicator dye of the $E_T(30)$ scale. The enhanced sensitivity of $E(F)$ compared to $E(A)$ towards change in the solvent polarity may be seen from the slope of the plot in Fig. 3b. This could be intelligible in terms of increased solute–solvent dipo-

Table 1
Photophysical parameters of the dye **1k** in different solvent media.

No.	Solvent	$E(A)$ ($\pm$0.04 kcal mol^{-1})	$E(F)$ ($\pm$0.06 kcal mol^{-1})	Φ_{fl}[a]	τ_0 (ns)	$k_r \times 10^7$ (s^{-1})	$k_{nr} \times 10^8$ (s^{-1})
1	DMSO	80.90	74.61	0.09	5.53	1.63	1.65
2	DMF	81.08	71.19	0.06	5.45	1.10	1.72
3	MeOH	82.49	75.12	0.06	4.09	1.47	2.30
4	Benzonitrile	93.37 82.82	66.33 61.59	0.38	4.09	9.29	1.52
5	EtOH	82.73	74.69 65.07	0.11	4.15	2.65	2.14
6	Acetone	83.69	74.84	0.41	4.45	9.21	1.33
7	2-Propanol	82.73	75.00 67.05	0.11	5.47	2.01	1.63
8	1-Butanol	82.73	75.08	0.09	5.18	1.74	1.76
9	THF	82.87	75.00 71.05 67.05	0.10	4.51	2.22	1.99
10	EtOAc	83.74	75.04	0.03	4.35	0.69	2.23
11	1,4-Dioxan	96.91 83.64	75.04 66.92	0.11	3.24	3.39	2.75

[a] The fluorescence of **1k** in different solvents were measured at O.D. 0.07 at the excitation wavelength 340 nm. The fluorescence quantum yields of **1k** were relative to those of the reported [10] values of quinine sulphate in 0.1M H_2SO_4.

lar interaction in the excited state. Solvents possessing nitrogen or oxygen centre available for electron donation to form hydrogen bond are expected to coordinate with the -enol form of **1k** in the excited state. Since the emission spectrum in benzonitrile shows a broad band at a much longer wavelength, the formation of hydrogen bonded solute–solvent complex in the excited state is indicated. This might also be similarly true for N,N-dimethyl formamide (DMF) and acetone. Thus it is expected that besides the non-specific dipolar interaction, specific hydrogen-bonding interaction plays a significant role in this solvatochromic effect.

Multiple linear regression analysis has been done where correlation of $E(A)$ or $E(F)$ was sought with respect to the solvatochromic parameters representing dipolarity (π^*), hydrogen bond donation (α, HBD) and hydrogen bond acceptance (β, HBA) ability of solvents (following the Taft's scale: π^*, α and β, respectively [22]). These were performed with the help of Eq. (2):

$$(E_x) = (E_x)_0 + A\alpha + B\beta + C\pi * + \cdots \quad (2)$$

where $(E_x)_0$ is the value of (E_x) in a hypothetical inert solvent, and A, B and C are the adjusted coefficients reflecting the dependence of E_x on the α, β and π^* solvent parameters. The following regression equations were obtained:

$$E(A) = 89.17 + 4.15\alpha - 17.41\beta + 5.25\pi * + \cdots; \quad (n = 11, \quad r = 0.72) \quad (3)$$

$$E(F) = 70.77 - 0.36\alpha + 7.99\beta - 3.25\pi * + \cdots; \quad (n = 11, \quad r = 0.42) \quad (4)$$

$$[E(\mathrm{St})] = 12.30 + 0.04\alpha - 9.17\beta + 4.03\pi * + \cdots; \quad (n = 11, \quad r = 0.64) \quad (5)$$

Although **1k** showed better correlation (r) of absorption energy $E(A)$ in terms of the Taft's π^*-, α- and β-parameters, the correlation coefficient (r = 0.42) was far from unity for $E(F)$ due to the low-solvatochromic shifts observed in the emission (Table 1), which has led to a higher dispersion of the experimental values. In our previous study [23] we have seen that pyromethene dyes also show similar correlation. The adjusted coefficient (B) describing the HBA ability of solvent was the major coefficient in all the three equations (3)–(5). For the energy of absorption as well as that of Stoke's shift, B coefficients had negative values, corroborating the observed bathochromic shift with respect to increasing solvent basicity, while for emission the shift was hypsochromic in nature and the coefficient (B) had positive sign. The reverse effect was observed as the acidity of solvent was increased. The coefficient (C) reflecting the dipolarity/polarizability of solvent took positive value in absorption and negative in case of emission, suggesting

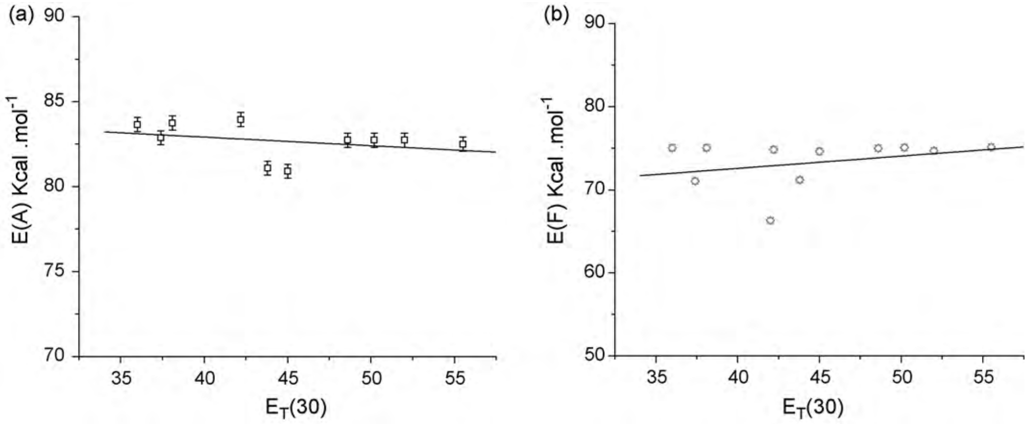

Fig. 3. Evolution of the absorption energy maxima (a) and emission energy maxima (b) of **1k** with the Reichardt global solvent parameter $E_T(30)$.

that the absorption bands shift slightly towards higher energies while the emission bands towards lower energies as the polarity of the solvent was increased. The solvent acidity coefficient (*A*) takes a sign opposite to that of the basicity coefficient (*B*), and its effect was much more prominent for the absorption and the Stoke's parameters as compared to that for emission. The acidity of solvent (α-scale) and dipolarity (π^*-scale) do not evidently affect the absorption and fluorescence maxima since the corresponding adjusted coefficients (*A* and *C* in Eqs. (3)–(5)) were within their standard deviations.

Compared to the steady state emission results (Table 1), the time-resolved emission data revealed a much weaker response to the emission characteristics by solvent polarity. The time-resolved data showed a highest lifetime (5.53 ns) of **1k** in DMSO, while in 1,4-dioxan it was 3.24 ns (*vide infra*). Thus, in solvents with a wide variation of polarities, the maximum difference in τ_0 was found to be ~2.3 ns. Exceptionally high emission quantum yields were obtained in benzonitrile and acetone. The radiative rate (k_r) of **1k**, calculated using the standard expression, $k_r = \Phi/\tau$ revealed a maximum value ($9.29 \times 10^7\ \mathrm{s}^{-1}$) in benzonitrile and a minimum value ($0.69 \times 10^7\ \mathrm{s}^{-1}$) in ethyl acetate, while in acetone the diketone had much higher k_r ($9.21 \times 10^7\ \mathrm{s}^{-1}$) values compared to the rest (Table 1). The stronger the ability of H-bonding in the excited state, the better quantum yield or radiative rate constants were observed, as reflected through the Taft's basicity (β-) scale. The non-radiative rate, $k_{\mathrm{nr}} = (1 - \Phi)/\tau$ was maximum in 1,4-dioxan and minimum in acetone.

It appeared here that solvation is mainly controlled through the dipolar interaction (π^*) and hydrogen bond acceptance (β) by the solvent. The ratio of the regression coefficients of β and π^* indicates the relative importance of HBA over dipolarity interaction. The ratio is ~ 3.5 in respect of $E(A)$, whereas it is about 2.5 for $E(F)$, implying that HBA plays a significantly greater role in the absorption. This result might be interpreted in terms of the tighter hydrogen bonding of the enolic hydrogen of **1k** with the solvent's electron rich centre in the ground state.

Typically the fluorophore has a larger dipole moment in the excited state (μ_{E}) than in the ground state (μ_{G}). Following excitation the solvent dipoles can reorient or relax around μ_{E} which lowers the energy of the excited state. As the solvent polarity is increased, this effect becomes stronger, resulting in emission at lower energies or longer wavelengths. This may be seen from the data in Table 1 that the emission energy in DMSO is smaller than that in Dioxan. Further, fluorescence lifetimes (1–10 ns) are usually much longer than the solvent relaxation time (10–100 ps) occurring at room temperature. The emitting probe is thus exposed to the solvent relaxed state which is distinctly different from the absorbing state. An important factor affecting emission includes specific solvent effects due to fluorophore–solvent interactions. We have observed here that the electron pair donating or hydrogen bond accepting ability of the solvent plays a pivotal role for the observed photophysical variation. This variation in stability of the excited state has a clear bearing on the lifetime which is discernible through our observation in Table 1.

3.2. Interaction with Mg^{+2} ion

3.2.1. Observation of CT bands

Absorption band maximum of **1k** in the aprotic polar acetone or in protic polar methanol shifted towards red as $Mg(ClO_4)_2$ was added to the solution (Fig. 4). Only the cation of the electrolyte has been found to be effective in the band shifts. Fig. 5 shows the electronic absorption spectra of mixtures containing **1k** + $Mg(ClO_4)_2$ in methanol and in acetone. To obtain these CT bands, spectra of above solutions were recorded against the pristine diketone (**1k**) solution in the respective solvent media as reference to cancel out its own absorbance. It was observed that new absorption peaks appeared in the visible region. The CT absorption spectra were characterized by fitting to the gaussian function:

$$y = y_0 + \left[\frac{A}{w\sqrt{(\pi/2 \quad \exp[-2(x - x_c)^2/w^2}} \right]$$

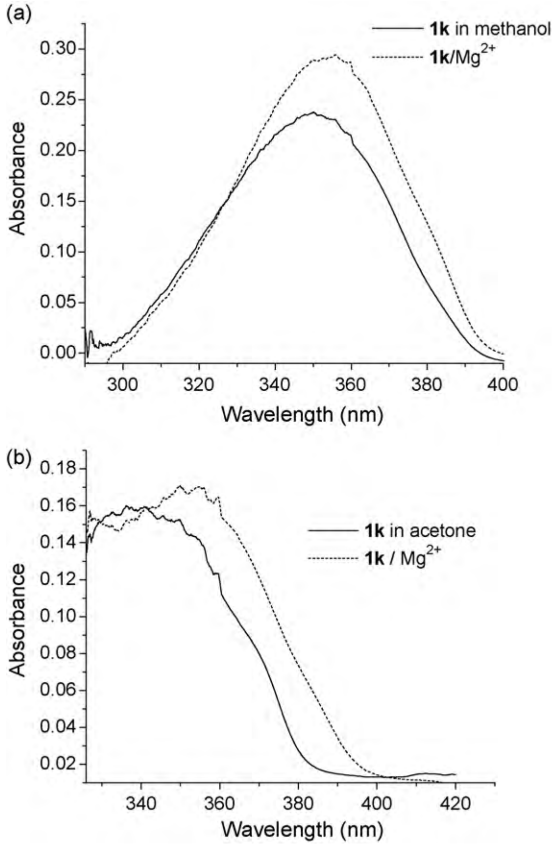

Fig. 4. Shifting of absorption maxima of (a) **1k** (1.339×10^{-5} mol dm^{-3}) in methanol on addition of Mg^{2+} (1.344×10^{-5} mol dm^{-3}) and of (b) **1k** (1.786×10^{-5} mol dm^{-3}) in acetone on addition of Mg^{2+} (9.85×10^{-5} mol dm^{-3}).

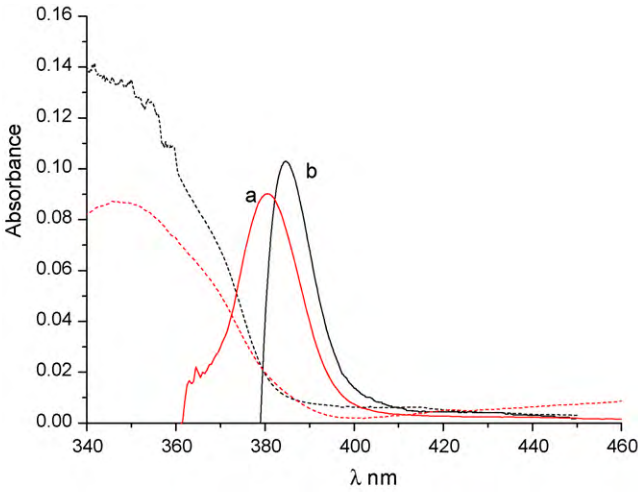

Fig. 5. Charge transfer absorption band of (a) Mg^{2+} (6.18×10^{-5} mol dm^{-3}) and **1k** (1.154×10^{-4} mol dm^{-3}) in methanol and (b) Mg^{2+} (2.814×10^{-4} mol dm^{-3}) and **1k** (1.276×10^{-4} mol dm^{-3}) in acetone against the pristine **1k** solution as reference.

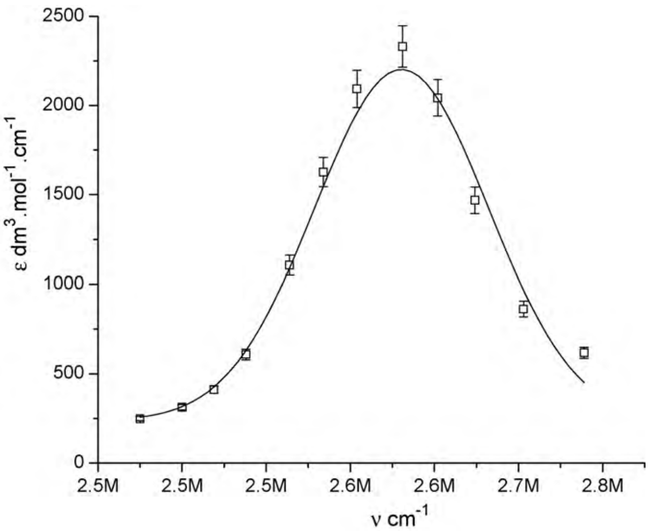

Fig. 6. Gaussian curve analysis of the CT band appeared in methanol.

Table 2
Gaussian curve analysis for the CT spectra of **1k** and $Mg(ClO_4)_2$ in methanol and acetone at temperature 303 K. CT absorption maxima, transition energies, oscillator strengths (f) and resonance energies (R_N) of the same complexes.

Parameters	**1k**/Mg^{+2} in methanol	**1k**/Mg^{+2} in acetone
Gaussian curve analysis data		
10^{-6} Area of the curve (A) ($dm^3\ mol^{-1}$)	254.81 ± 6.48	765.43 ± 163.93
Width of the curve (w) (cm^{-1})	1032.08 ± 23.85	2939.68 ± 2238.71
Center of the curve (x_c) (cm^{-1})	26304.58 ± 10.30	25672.88 ± 14.86
y_0 ($dm^3\ mol^{-1}\ cm^{-1}$)	236.07 ± 13.79	-1592.842 ± 2873.643
λ_{CT} (nm)	380.16	389.00
$h\nu_{CT}$ (eV)	3.2623	3.1882
f ($dm^3\ mol^{-1}\ cm^{-2}$)	1.361	0.2545
$\lvert R_N \rvert$ (eV)	0.0770	0.02845

where x and y denote wavenumber and molar extinction coefficient respectively. One such plot has been shown in Fig. 6. The results of the Gaussian fit for the **1k**/Mg^{2+} system in both the solvent media under study were shown in Table 2. The wavelengths at these new absorption maxima ($\lambda_{max} = x_c$) and the corresponding transition energies ($h\nu$) were summarized in Table 2. The gaussian analysis of fitting was done in accordance with the method developed by Gould et al. [24]. Polar solvents were chosen primarily to achieve practical levels of solubility, but additionally this serves another important purpose. Within an excellent solvent media containing the metal perchlorate and **1k**, any **1k**/Mg^{2+} interaction has to compete with **1k**/solvent interaction. The ultimate demonstration of **1k**/Mg^{2+} binding in both methanol and acetone media might therefore be considered as an evidence for their spontaneous attraction.

A protic solvent, methanol does not find enough chance to form hydrogen bond with the carbonyl oxygen of **1k** since the 6-membered -enol form (Fig. 1) gains extra stability due to intramolecular hydrogen bonding. In the aprotic dipolar acetone, a better intermolecular interaction takes place between the solute **1k** and the surrounding solvent dipoles. Both the polar solvents methanol and acetone attempted to stabilise the enol form of **1k** through intermolecular hydrogen bonding with the enolic proton, competing against the intrinsic tendency of **1k** to form intramolecular H-bonded ring structure. This tendency was stronger in the case of aprotic acetone. With the addition of an electrolyte to **1k** solution in methanol medium, the positively charged cation competes for replacement either with the protic hydrogen of methanol or with the enolic proton of **1k** for enjoying better interaction with the negative oxygen centre either in the solvent or in the carbonyl oxygen of the diketone molecule. However, on addition of the electrolyte, the Mg^{2+}, cation refuses the solvent molecule and preferentially engages in the position of the enolic proton thus invoking a weak interaction between the metal ion and the carbonyl oxygen of the **1k** molecule. Formation of diketone–cation complex is also rationalizable in terms of small size and stronger Lewis acidity of Mg^{2+} ion. The absorption band is supposed to originate from a $\pi \rightarrow \pi^*$ transition with a significant transfer of charge from the O-atom of one carbonyl group to the other carbonyl oxygen attached to Mg^{2+} ion in the molecule. The dipolemoment of **1k** in the excited (S_1) state has been found to be greater than that in the ground state. Thus, greater the interaction of the diketone with the surrounding molecules, the greater is the red shift of the absorption band. Our experimental results indicated that **1k**–Mg^{2+} ion interactions were greater than **1k**–solvent interaction.

From the CT absorption spectra, we could estimate oscillator strength (f) for the transition [25]. The observed oscillator strengths of the CT bands are summarized in Table 2. The oscillator strength (f) is proportional to the square of transition dipole $|\mu_i|^2$. The higher observed oscillator strength of the **1k**/Mg^{+2} complex in methanol as recorded in Table 2 might reflect the higher transition dipole where there is enough scope for stable intramolecular 6-membered ring formation. In case of acetone there must be smaller values of transition dipole might be because of intermolecular stabilization of the metal-complex involving the surrounding dipolar acetone solvent through its electron donating oxygen centre.

Again the resonance energy of the complex in the ground state (R_N) [26] obviously, is a contributing factor to the stability of the complex (a ground state property). The values of R_N for the complexes under study have been provided in Table 2. Trend in R_N values show that Mg^{2+} forms stronger complex with **1k** in protic polar methanol medium as compared to the aprotic acetone.

Table 3
Data for spectrophotometric determination of stoichiometry, formation constants (K) and molar absorptivities (ε) of the **1k**/Mg^{+2} complexes in methanol and in acetone at temperature = 298 K.

Solvent media	$[Mg^{+2}]$ ($mol.dm^{-3}$)	$[\mathbf{1k}]_0$ ($mol\ dm^{-3}$)	Absorbance at λ_{CT}	$K \times 10^{-5}$ ($dm^3\ mol^{-1}$)	$\varepsilon \times 10^{-3}$ ($dm^3\ mol^{-1}\ cm^{-1}$)
Methanol	4.480×10^{-5}	1.339×10^{-5}	0.0581	1.265 ± 0.157	4.562
	8.960×10^{-5}		0.0526		
	1.344×10^{-4}		0.0562		
	1.792×10^{-4}		0.060		
	2.240×10^{-5}		0.0650		
Acetone	9.850×10^{-5}	1.786×10^{-5}	0.0380	1.182 ± 0.809	2.350
	1.970×10^{-4}		0.0415		
	2.955×10^{-4}		0.0417		
	3.940×10^{-5}		0.0387		
	4.925×10^{-5}		0.0414		

Table 4
Formation constants (K dm^3 mol^{-1}) and thermodynamic parameters (ΔH_f^0 kcal mol^{-1}, ΔS_f^0 cal mol^{-1} K^{-1} and ΔG_f^0 kcal mol^{-1}) for the **1k**/Mg^{2+} adduct at four different temperatures in methanol and in acetone.

Solvent	Temperature (K)	K (dm^3 mol^{-1})	ΔH_f^0 (kcal mol^{-1})	ΔS_f^0 (cal mol^{-1} K^{-1})	ΔG_f^0 (kcal mol^{-1})
Methanol	298	$1.2648 \times 10^5 \pm 1.572 \times 10^4$	-23.34 ± 1.96	55.07 ± 6.41	-6.929 ± 0.05
	303	$5.4430 \times 10^4 \pm 1.361 \times 10^4$			-6.651 ± 0.02
	308	$2.9127 \times 10^4 \pm 0.075 \times 10^4$			-6.378 ± 0.014
	313	$1.7739 \times 10^4 \pm 1.842 \times 10^3$			-6.103 ± 0.05
Acetone	298	$1.1824 \times 10^5 \pm 8.093 \times 10^4$	-36.73 ± 4.63	99.58 ± 15.11	-7.055 ± 0.13
	303	$7.26 \times 10^4 \pm 2.391 \times 10^4$			-6.557 ± 0.051
	308	$1.8867 \times 10^4 \pm 8.642 \times 10^3$			-6.059 ± 0.024
	313	$6.2550 \times 10^3 \pm 5.188 \times 10^2$			-5.561 ± 0.099

3.2.2. *Determination of formation constants (K)*

The formation constant of the **1k**/Mg^{2+} complex has been determined using the well known [25] Benesi–Hildebrand (BH) [27] equation. The intensity in the visible portion of the absorption band, measured against the solvent as reference, increases systematically with gradual addition of Mg(ClO$_4$)$_2$. Thus, it is sufficiently established in this work that the substantial red shift in the broad 300–400 nm absorption band of **1k** is due to formation of 1:1 molecular complex between Mg^{2+} and **1k**. This observation points to complex formation. The equilibrium constant values were calculated using the BH model. In all the cases very good linearity were obtained.

The following linear regression equations have been obtained with the present data:

In methanol at 303 K:

$$\frac{[1k]_0[Mg^{+2}]_0}{d} = \frac{[Mg^{+2}]_0}{67.94 \times 10^2} + 37.018 \times 10^7 \quad (r = 0.99) \tag{6}$$

In acetone at 303 K:

$$\frac{[1k]_0[Mg^{+2}]_0}{d} = \frac{[Mg^{+2}]_0}{81.97 \times 10} + 59.52 \times 10^6 \quad (r = 0.92) \tag{7}$$

Formation constants for the complexes at 298 K of **1k** with Mg^{2+} in methanol and in acetone were summarized in Table 3. It is observed that **1k** binds more strongly with Mg^{2+} in methanol rather than in acetone more or less at all the temperatures in the studied range.

3.2.3. *Determination of the thermodynamic parameters (ΔH_f^0, ΔS_f^0 and ΔG_f^0)*

Binding constants were determined through Benesi–Hildebrand equation at four different temperatures and then the enthalpy, entropy and the free energies of the complex formation from vant Hoff's equation.

The following linear regression equations have been obtained with the present data: In methanol:

$$\ln K = \frac{11.67 \times 10^3}{T} + [-27.53] \quad (r = 0.99) \tag{8}$$

In acetone:

$$\ln K = \frac{18.37 \times 10^3}{T} + [-49.79] \quad (r = 0.98) \tag{9}$$

For **1k**/Mg^{2+} system the binding constants values at four different temperatures were shown in Table 4. It might be seen that enthalpies of formation follow the order ΔH_f^0 (methanol) < ΔH_f^0 (acetone) along with a similar trend for entropy of formation (ΔS_f^0). But Gibb's free energy of formation (ΔG_f^0) shows clearly that at all temperature MeOH was found to be the favourable medium for Mg^{2+} to form complex with **1k** over AC.

3.2.4. *Fluorescence quenching behaviour*

The diketone **1k** exhibits distinct fluorescence characteristics with emission maxima in the range 375–425 nm (Fig. 2) in various solvents. In fluorescence quenching study (Fig. 7a) it was observed that on addition of Mg(ClO$_4$)$_2$ to the **1k** solution in acetone medium, the pattern of the emission spectrum changed entirely to that in the non-polar tetrahydrofuran (THF) medium, with simultaneous quenching of intensity. In methanol medium (Fig. 7b) the spectral pattern remains almost unchanged while there was quenching in fluorescence intensity alone.

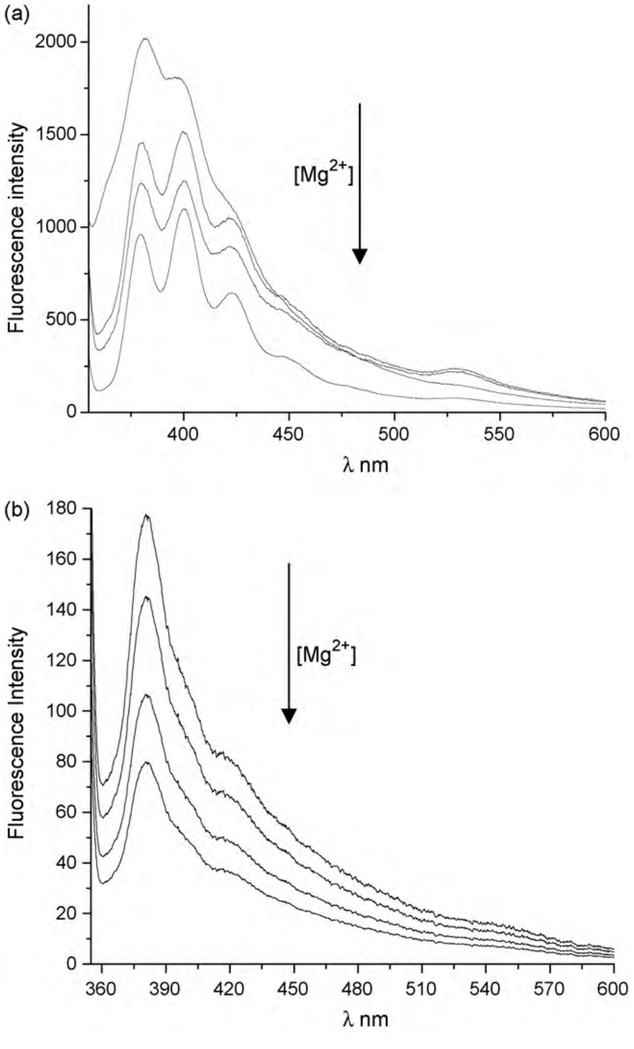

Fig. 7. (a) Fluorescence quenching of **1k** (1.786×10^{-5} mol dm^{-3}) in acetone on gradual addition of Mg(ClO$_4$)$_2$, from top to bottom concentration of Mg^{2+} (0.00 mol dm^{-3}), (9.85×10^{-5} mol dm^{-3}), (1.97×10^{-4} mol dm^{-3}) and (2.95×10^{-4} mol dm^{-3}). (b) Fluorescence quenching of **1k** (1.339×10^{-5} mol dm^{-3}) in methanol on gradual addition of Mg(ClO$_4$)$_2$, from top to bottom concentration of Mg^{2+} (0.00 mol dm^{-3}), (4.480×10^{-5}mol dm^{-3}), (8.960×10^{-5}mol dm^{-3}) and (1.344×10^{-4}mol dm^{-3}).

In interpreting this observation, we have proposed that the diketone (**1k**) exists in solution in both intra- and intermolecular hydrogen bonded forms. Since its 6-membered enol form gains extra stability due to intramolecular hydrogen bonding, the protic solvent molecules cannot effectively enter into hydrogen bonding with the carbonyl oxygen of **1k**. Thus the hydrogen donor protic solvents (alcohols, etc.) fail to compete with the aprotic electron donating (hydrogen accepting) solvents like benzonitrile, acetone, DMF, etc. in forming the intermolecular H-bond with **1k**. The enolic proton, a member of the 6-membered ring structure, plays a pivotal role in choosing solvent molecule for intermolecular H-bonding. This fluorescence interaction study clearly indicates that the solute–solvent hydrogen bonding, which is gradually lost with addition of $Mg(ClO_4)_2$, was dominantly present with aprotic acetone but absent in protic methanol. This is precisely what we have investigated in the solvatochromatic study, the electron pair donating ability or hydrogen bond accepting ability or rather basicity of solvent is the key factor for these photophysical variations.

Thus by breaking the inter- and subsequently the intramolecular H-bonds, Mg^{2+} secures position to form complex with the keto- form of **1k** in aprotic solvents like acetone. The ground state complex **1k**/Mg^{2+} in acetone is stabilized due to intermolecular interaction take place between magnesium ion and the electron donating solvent which is not the situation for H-donating methanol. This possibly results in the higher enthalpy as well as entropy of complexation in acetone rather than in methanol.

4. Conclusion

(1) Energy of maximum absorption and emission of the diketone (**1k**) depend significantly on the basicity of solvent media rather than on polarity or acidity, and this is predominant in the ground state.
(2) The Stokes shift in aprotic solvents is assigned to the hydrogen bonding of the solute's enolic hydrogen binding with the solvent's electron donor centres; this property makes this class of diketone a suitable 'probe' for studying hydrogen-bonding characteristics in mixed binary (protic–aprtic) solvents.
(3) Absorption spectral studies point to the formation of a cation–diketone complex in the ground (S_0) state.
(4) Steady state emission studies indicate that in the solution phase both inter- and intramolecular hydrogen bonding exists.
(5) Both enthalpy and entropy of complex formation of **1k** with Mg^{2+} ions is greater in aprotic acetone media than in the protic methanol.

References

[1] A. Baeyer, V. Villiger, Dibenzalaceton und triphenylmethan, Ein Beitrag zur Farbtheorie. Ber. Dtsch. Chem. Ges. 35 (1902) 1189–1201.
[2] E.M. Kosower, The effect of solvent on spectra. III. The use of *Z*-values in connection with kinetic data, J. Am. Chem. Soc. 80 (1958) 3261–3267.
[3] C. Reichardt, Solvatochromic Dyes as Solvent Polarity Indicators, Chem. Rev. 94 (1994) 2319–2358, and references there in.
[4] M.C. Rezende, D. Zanette, C. Zucco, A general empiral equation for salt effects, Tetrahedron Lett. 25 (1984) 3423–3424.
[5] M.C. Rezende, The polarity of alcoholic electrolyte solutions: a systematic study, Tetrahedron 44 (1988) 3513–3522.
[6] C. Reichardt, S. Asharin-Fard, G. Schafer, Pyridinium *N*-phenoxide betaines and their application to the characterization of solvent polarities, XIX. The halochromism of pyridinium *N*-phenoxide betaine dyes in acetonitrile solution, Chem. Ber. 126 (1993) 143–147.
[7] D.A. Binder, M.M. Kreevoy, Interaction of Li^+ with phenoxide ions in acetonitrile, J. Phys. Chem. 98 (1994) 10008–10016.
[8] S. Zanotto, C.M. Scremin, C. Machado, M.C. Rezende, Cationic and anionic halochromism, J. Phys. Org. Chem. 6 (1993) 637–641.
[9] P.A. Thompson, J.D. Simon, Electrolyte effects on molecular radiationless decay: The photophysics of 3-aminofluorenone in acetonitrile-salt solutions, J. Chem. Phys. 97 (1992) 4792–4799.
[10] G. Zhang, S.H. Kim, R.E. Evans, B.H. Kim, J.N. Demas, C.L. Fraser, Luminescent donor–acceptor β-diketones: modulation of emission by solvent polarity and Group II metal binding, J. Fluoresc. 19 (2009) 881–889.
[11] C. Pettinari, F. Marchetti, A. Drozdov, β-Diketones and related ligands, Coord. Chem. Rev. II 1 (2003) 97–115.
[12] E. DeOliveira, C.R. Neri, O.A. Serra, A.G.S. Prado, Antenna effect in highly luminescent Eu^{3+} anchored in hexagonal mesoporous silica, Chem. Mater. 19 (2007) 5437–5442.
[13] P. Banet, L. Legagneux, P. Hesemann, J.J.E. Moreau, L. Nicole, A. Quach, C. Sanchez, T.H. Tran-Thi, Hybrid mesostructured thin films functionalized with DBM as new selective sensors of BF_3, Sens. Actuators B Chem. 130 (2008) 1–8.
[14] W. Huang, J. Wang, Q. Shen, X. Zhou, An efficient $Yb(OTf)_3$ catalyzed alkylation of 1,3-dicarbonyl compounds using alcohols as substrates, Tetrahedron Lett. 48 (2007) 3969–3973.
[15] J.A. Cowan, Biological Chemistry of Magnesium, VCH, New York, 1995.
[16] M.J. Berridge, M.D. Bootman, H.L. Roderick, Calcium signalling: dynamics, homeostasis and remodelling, Nat. Rev. Mol. Cell Biol. 4 (2003) 517–529.
[17] V Goldschmidt, J. Didierjean, B. Ehresmann, C. Ehresmann, C. Isel, R. Marquet, Mg^{2+} dependency of HIV-1 reverse transcription, inhibition by nucleoside analogues and resistance, Nucleic Acids Res. 34 (2006) 42–52.
[18] T. Kirschberg, J. Parrish, Metal chelators as antiviral agents, Curr. Opin. Drug Discov. Dev. 10 (2007) 460–472.
[19] E.J. Park, M. Brasuel, C. Behrend, M.A. Philbert, R. Kopelman, Ratiometric optical PEBBLE nanosensors for real-time magnesium ion concentrations inside viable cells, Anal. Chem. 75 (2003) 3784–3791.
[20] R. Rudolf, M. Mongillo, R. Rizzuto, T. Pozzan, Innovation: looking forward to seeing calcium, Nat. Rev. Mol. Cell Biol. 4 (2003) 579–586.
[21] X. Zhang, Z.-C. Li, N. Xu, K.-B. Li, S. Lin, F.-Z. Lu, F.-S. Du, F.-M. Li, β-Diketones bearing electron-donating chromophores and a novel β-triketone: synthesis and reversible fluorescence behavior, Tetrahedron Lett. 47 (2006) 2623–2626.
[22] M.J. Kamlet, R.W. Taft, The solvatochromic comparison method. I. The beta-scale of solvent hydrogen-bond acceptor (HBA) basicities, J. Am. Chem. Soc. 98 (1976) 377–383.
[23] T. Chaudhuri, S. Mula, S. Chattopadhyay, M. Banerjee, Photophysical properties of the 8-phenyl analogue of PM567: a theoretical rationalization, Spectrochim. Acta A: Mol. Biomol. Spectrosc. 75 (2010) 739–744.
[24] I.R. Gould, D. Noukakis, L. Gomez-Jahn, R.H. Young, J.L. Goodman, S. Farid, Radiative and nonradiative electron transfer in contact radical–ion pairs, Chem. Phys. 176 (1993) 439–456.
[25] S. Bhattacharya, S. Bhattacharya (Banerjee), K. Ghosh, S. Basu, M. Banerjee, Study of electron donor–acceptor complex formation of *o*-chloranil with a series of phosphine oxides and tri-*n*-butyl phosphate by the absorption spectrometric method, J. Solution Chem. 35 (2006) 519–539.
[26] G. Briegleb, J. Czekalla, Intensity of electron transition bands in electron donator-acceptor complexes, Z. Physik. Chem. (Frankfurt) 24 (1960) 37–54.
[27] H.A. Benesi, J.H. Hildebrand, A spectrophotometric investigation of the interaction of iodine with aromatic hydrocarbons, J. Am. Chem. Soc. 71 (1949) 2703–2707.